Pleiotropic antitumor effects of the pan-HDAC inhibitor ITF2357 against c-Myc-overexpressing human B-cell non-Hodgkin lymphomas

Roberta Zappasodi[1], Alessandra Cavanè[1], Marilena V. Iorio[2], Monica Tortoreto[3], Carla Guarnotta[4], Giusi Ruggiero[1], Claudia Piovan[2], Michele Magni[1], Nadia Zaffaroni[3], Elda Tagliabue[5], Carlo M. Croce[6], Franco Zunino[3], Alessandro M. Gianni[1,7] and Massimo Di Nicola[1]

[1] Medical Oncology Department, Fondazione IRCCS Istituto Nazionale per lo Studio e la Cura dei Tumori, Milan, Italy

[2] Start Up Unit, Molecular Targeting Unit, Fondazione IRCCS Istituto Nazionale per lo Studio e la Cura dei Tumori, Milan, Italy

[3] Molecular Pharmacology Unit, Fondazione IRCCS Istituto Nazionale per lo Studio e la Cura dei Tumori, Milan, Italy

[4] Tumor Immunology Unit, Department of Health Science, Human Pathology Section, School of Medicine, University of Palermo, Palermo, Italy

[5] Molecular Targeting Unit, Fondazione IRCCS Istituto Nazionale per lo Studio e la Cura dei Tumori, Milan, Italy

[6] Department of Molecular Virology, Immunology and Medical Genetics, Ohio State University, Columbus, OH

[7] Medical Oncology, University of Milan, Milan, Italy

Histone deacetylases (HDAC) extensively contribute to the c-Myc oncogenic program, pointing to their inhibition as an effective strategy against c-Myc-overexpressing cancers. We, thus, studied the therapeutic activity of the new-generation pan-HDAC inhibitor ITF2357 (Givinostat®) against c-Myc-overexpressing human B-cell non-Hodgkin lymphomas (B-NHLs). ITF2357 anti-proliferative and pro-apoptotic effects were analyzed in B-NHL cell lines with c-Myc translocations (Namalwa, Raji and DOHH-2), stabilizing mutations (Raji) or post-transcriptional alterations (SU-DHL-4) in relationship to c-Myc modulation. ITF2357 significantly delayed the *in vitro* growth of all B-NHL cell lines by inducing G1 cell-cycle arrest, eventually followed by cell death. These events correlated with the extent of c-Myc protein, but not mRNA, downregulation, indicating the involvement of post-transcriptional mechanisms. Accordingly, c-Myc-targeting microRNAs let-7a and miR-26a were induced in all treated lymphomas and the cap-dependent translation machinery components 4E-BP1, eIF4E and eIF4G, as well as their upstream regulators, Akt and PIM kinases, were inhibited in function of the cell sensitivity to ITF2357, and, in turn, c-Myc downregulation. *In vivo*, ITF2357 significantly hampered the growth of Namalwa and Raji xenografts in immunodeficient mice. Noteworthy, its combination with suboptimal cyclophosphamide, achieved complete remissions in most animals and equaled or even exceeded the activity of optimal cyclophosphamide. Collectively, our findings provide the rationale for testing the clinical advantages of adding ITF2357 to current therapies for the still very ominous c-Myc-overexpressing lymphomas. They equally provide the proof-of-concept for its clinical evaluation in rational combination with the promising inhibitors of B-cell receptor and PI3K/Akt/mTOR axis currently in the process of development.

Cancer Cell Biology

Deregulated expression of c-Myc transcription factor plays a critical role in the pathogenesis and progression of aggressive B-cell NHLs (B-NHLs) and multiple myeloma.[1,2] The prime example of c-Myc-driven oncogenesis is Burkitt's lymphoma (BL), a highly aggressive and fast-growing B-NHL, in which chromosomal translocations juxtaposing c-Myc with the promoter regions of immunoglobulin (Ig)-coding genes are virtually invariant, early oncogenic events.[3] Although the prognosis of BL has been significantly ameliorated by intensive chemotherapy regimens,[4] treatment-related toxicity is still a significant problem.[4,5] In addition, accumulating evidence is showing that c-Myc overexpression also defines a subgroup of aggressive B-NHLs across different histotypes, including transformed follicular, marginal zone, mantle cell and diffuse large B-cell lymphomas (DLBCL), with an extremely poor prognosis due to enhanced chemoresistance and aggressiveness.[1,6–8] This points to the urgent need for novel and more effective treatments for these diseases.

What's new?

c-Myc plays a critical role in aggressive B-cell non-Hodgkin lymphomas and multiple myelomas, and is associated with extremely poor prognosis. It hasn't been easy, though, to directly inhibit c-Myc. In this study, the authors found that a histone-deacetylase inhibitor (HDAC) called ITF2357 down-regulated c-Myc protein expression, and that microRNAs (miRNAs) may be involved. ITF2357 also significantly enhanced chemotherapy against human Burkitt's lymphoma in mice. These results suggest that indirectly interfering with c-Myc's oncogenic functions is a promising therapeutic strategy, and that ITF2357 may be a valuable addition to conventional treatments for c-Myc-overexpressing lymphomas.

The clear causative role of c-Myc overexpression in B-cell lymphomagenesis[9,10] and its frequent association with an unfavorable prognosis[6,7] indicate that interfering with c-Myc's oncogenic functions may secure a better outcome. c-Myc is unique in its ability to bind approximately 10–15% of all human genes,[11] where it controls transcription via recruitment of specific co-activators or co-repressors, such as, respectively, histone acetyl-transferase (HATs)[12] or DNA methyltransferase and histone deacetylases (HDACs).[13–16] The transforming potential of c-Myc overexpression stems from its functions to promote cell proliferation, alter cell metabolism and favor genomic instability. For this reason, its expression is normally kept under tight control by several safeguard mechanisms, whose evasion/inactivation is a prerequisite for c-Myc-driven lymphomagenesis.[17,18]

Although several lines of evidence have established c-Myc as a reliable lymphoma therapeutic target,[10,19] strategies for its direct inhibition have not yet been successful probably because of the lack of a clear ligand-binding domain. The current understanding that c-Myc oncogenic gene expression reprogramming mostly relies on epigenetic changes makes HDAC inhibitors novel suitable drug candidates for the treatment of c-Myc-overexpressing lymphomas. This view has been further strengthened by recent demonstrations of their ability to downregulate c-Myc expression itself in different oncotypes, including Hodgkin lymphoma.[20,21] However, whether and how HDAC inhibitors can achieve this effect also in human c-Myc overexpressing (c-Myc+) B-cell NHLs as well as the resulting therapeutic impact against these diseases have not yet been specifically investigated.

Therefore, we looked to see whether HDAC pan-inhibition by the new-generation hydroxamate derivative ITF2357 (Givinostat®) was able to counteract c-Myc oncogenic functions in preclinical human c-Myc+ B-NHL models, and could thus constitute a useful addition to the treatment armamentarium for these diseases. In line with our hypothesis, we found that ITF2357 antiproliferative activity was proportional to c-Myc down-modulation in c-Myc+ B-NHL models. Interestingly, c-Myc reduction was limited to its protein levels and occurred independently from the presence of a *C-MYC-IG* translocation, indicating the involvement of post-transcriptional mechanisms. In view of the crucial bidirectional interplay between c-Myc and microRNAs (miRNAs), in particular let-7a and miR-26a,[22–24] and the requirement of cap-dependent translation initiation machinery[25] to ensure constitutive high levels of c-Myc protein expression, we specifically tested whether ITF2357 could affect these molecules. We found that let-7a and miR-26a were induced and cap-dependent translation initiation machinery inhibited after treatment, thus contributing to explain the persistent down-modulation of c-Myc protein. In two mouse models of human BL, ITF2357 provided the same molecular effects and significantly enhanced the therapeutic activity of cyclophosphamide (CTX), leading to long-lasting complete responses. Taken as a whole, these findings strongly highlight the therapeutic advantages of ITF2357 to concurrently abrogate multiple oncogenic pathways regulating c-Myc expression in c-Myc+ B-NHLs. They equally provide the proof-of-concept for its clinical evaluation in rational combination with available anticancer agents to improve the treatment of these diseases.

Material and Methods

Cells lines

Human B-NHL cell lines Namalwa (BL), Raji (BL), SU-DHL-4 (DLBCL) and DOHH-2 (*C-MYC-IG* translocated follicular lymphoma [FL]) (DSMZ, Braunschweig, Germany) were cultured in RPMI 1640 medium (Lonza, Switzerland) supplemented with 10% (volume/volume) inactivated FBS (Lonza) and 1% (volume/volume) L-glutamine (Lonza) in a humidified chamber with 5% CO_2 at 37°C. Viable cells in treated and untreated cultures were measured with the trypan blue exclusion test.

Drugs

ITF2357 (diethyl-[6-(4-hydroxycarbamoyl-phenyl carbamoyloxymethyl)-naphthalen-2-yl methyl]-ammonium chloride; monohydrate; Italfarmaco, patent WO 97/43251, US 6034096) was kindly provided by Italfarmaco (Milan, Italy). CTX was from Baxter (Endoxan, Baxter).

Flow cytometry analyses

Flow cytometry of apoptosis and the cell cycle were performed as previously described.[26,27]

For c-Myc intracellular staining, cells were treated with fixation and permeabilization buffers (eBioscience San Diego, CA) and incubated with a rabbit anti-human c-Myc monoclonal antibody (mAb) (Cell Signaling Technology), and a FITC-labeled goat anti-rabbit IgG (KPL) as a secondary Ab. Healthy donor peripheral blood mononuclear cell (PBMC) samples were stained with APC-labeled anti-human CD19
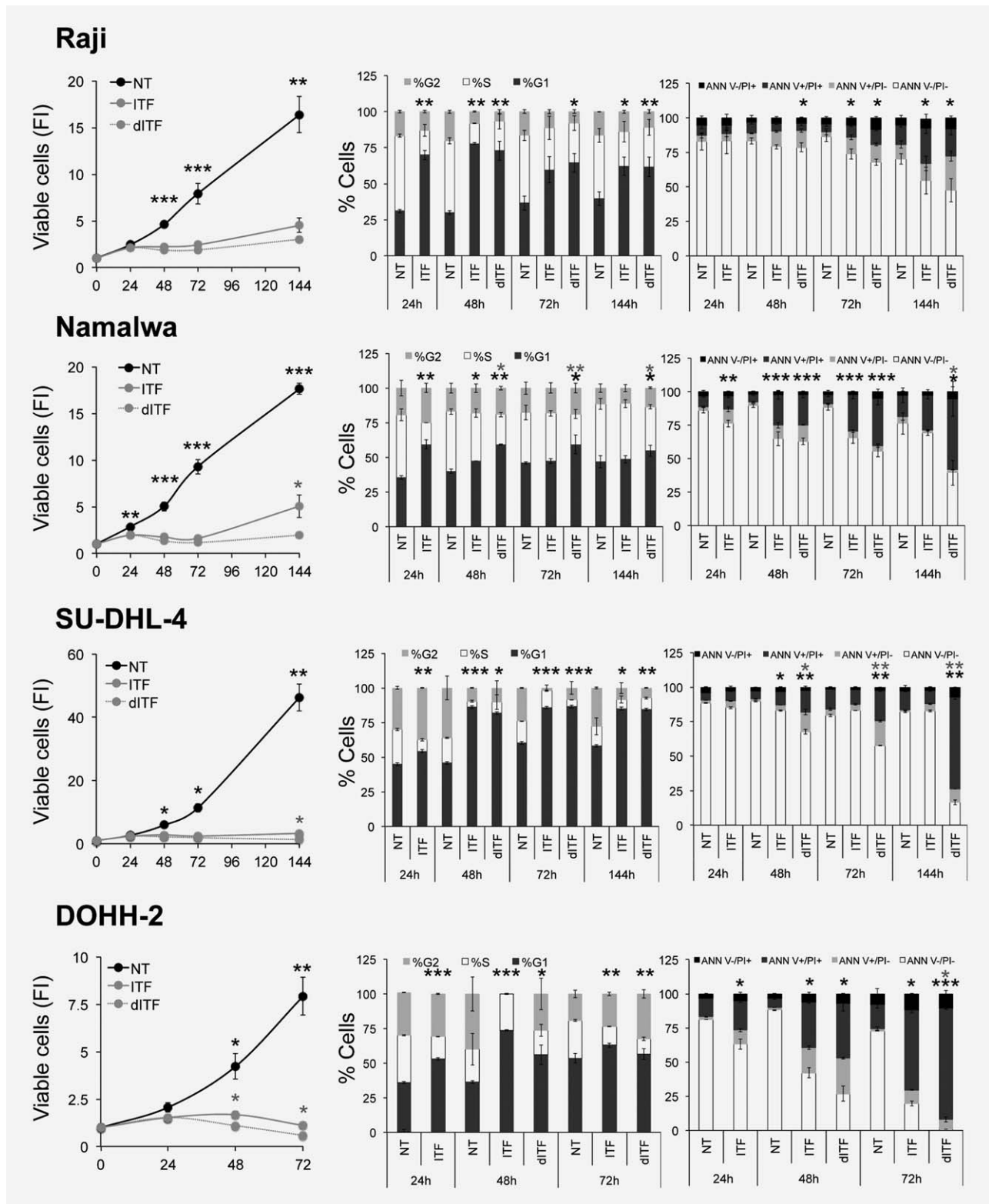
Figure 1. Cytotoxic and cytostatic effects of ITF2357 in c-Myc+ B-NHL cultures. Raji, Namalwa, SU-DHL-4 and DOHH-2 cells were incubated for the indicated period (hr) with 0.2 μM ITF2357 supplied as a single (ITF) or a daily treatment (dITF), or were not treated (NT) as control, and cell proliferation (left), cell-cycle progression (middle) and apoptosis induction (right) were assessed in culture at 24-hr intervals. Cell proliferation is represented as fold increase (FI) in viable cells with respect to the seeded cell number (left). Frequencies of cells in G1 (dark gray), S (white) and G2 (light gray) cell-cycle phases measured by flow cytometry are shown as histograms (middle). Apoptosis levels in treated or untreated cultures were determined by flow cytometry analysis of annexin V (ANN V) and PI co-staining (white, viable ANN V-PI-cells %; light gray, early apoptotic ANN V+PI− cells %; dark gray, late apoptotic ANN V+PI+ cells % and black, necrotic ANN V−PI+ cells %) (right). Data are the mean ± SE of at least four independent experiments. Statistically significant differences between treated and untreated cells (black asterisks) or between ITF and dITF treatments (gray asterisks) within the same time point were assessed with the unpaired two-tailed Student's *t* test (*$P < 0.05$; ** $P < 0.01$; *** $P < 0.001$).
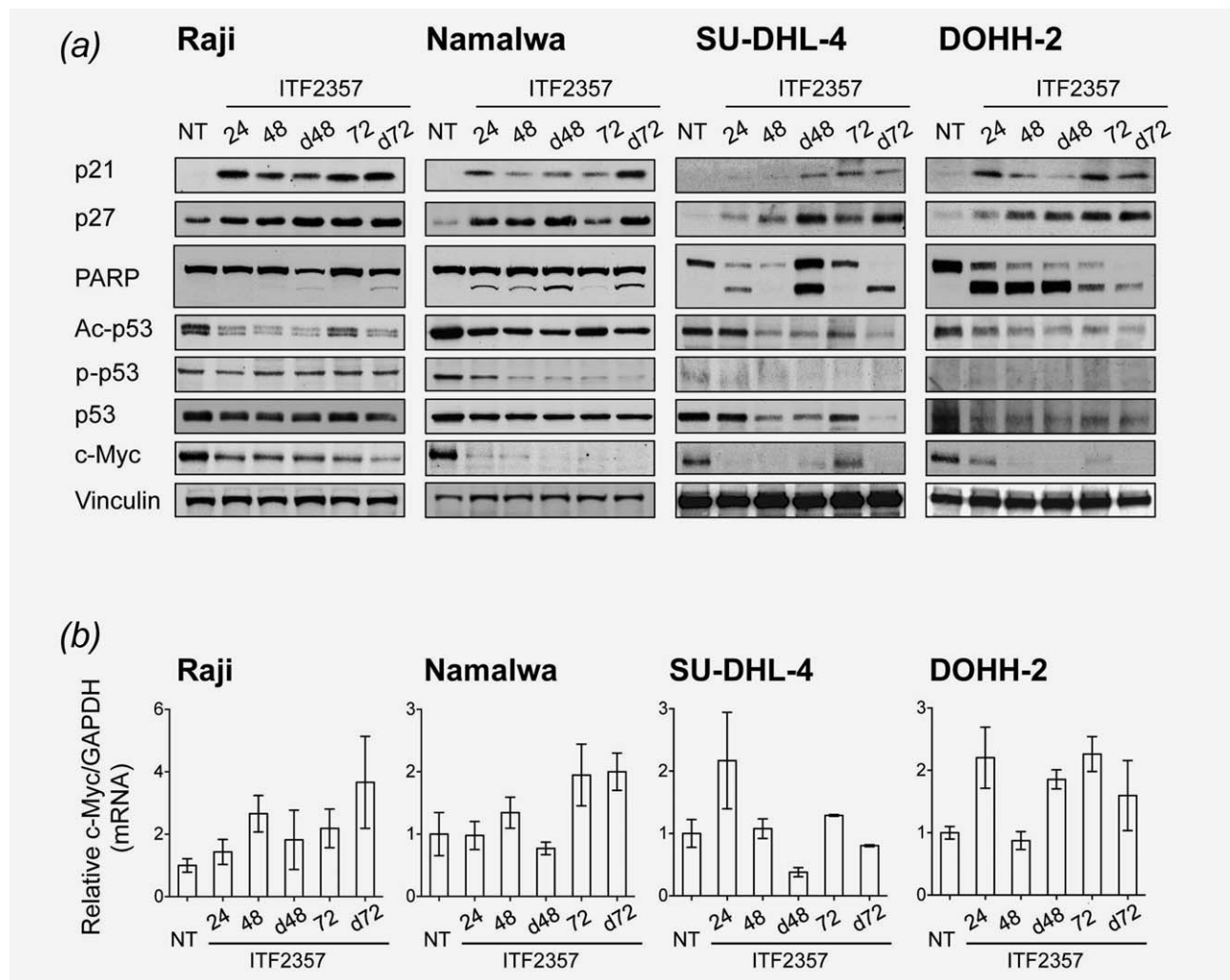
Figure 2. Expression analysis of molecular pathways associated with ITF2357 anti-lymphoma activity. (*a*) Representative western blot analyses of the indicated proteins in Raji, Namalwa, SU-DHL-4 and DOHH-2 cells cultured in the absence (NT) or presence of 0.2 μM ITF2357 administered once or every 24 hr (daily, d) for the indicated hours. Cellular vinculin content is shown as an internal protein loading control. Images were acquired by using Microtek ArtixScan F1, and cropped to retain the relevant bands with Adobe Photoshop CS version 4 for Macintosh computer. (*b*) Relative c-Myc mRNA expression levels measured by qRT-PCR in the same culture conditions described in (*a*). In each condition, c-Myc mRNA levels, upon normalization relative to GAPDH transcript, are expressed as fold change with respect to untreated cultures at any time point. Data are the mean ± SE of five independent experiments.

mAb (BD Biosciences) before being processed for c-Myc intracellular staining.

Data were acquired on a BD FACSCalibur using BD CellQuest software version 3.3 (Becton Dickinson) and analyzed by FlowJo 8.8.7 software version for Macintosh (Tree Star).

Western blot analyses

Lymphoma cells were solubilized in Laemli buffer as previously described,[26] or in RIPA buffer (Cell Signaling Technology), according to the manufacturer's instructions.

Histones extraction was performed by lysing cells in PBS containing 0.5% v/v Triton X 100, 2 mM phenylmethylsulfonyl fluoride, 0.02% w/v NaN, for 10 min on ice. After centrifugation at 6,500×*g* for 10 min, nuclear pellets were washed in lysis buffer and incubated overnight at 4°C in 0.2 N HCl.

Histones were recovered in the supernatant after centrifugation at 6,500×*g* for 10 min.

Western blotting was performed as already reported[26] by using primary Abs directed against the following human proteins: α-tubulin (1:2,000) (Invitrogen), p21 (1:1,000), p27 (1:1,000) and phosphorylated(p)-4E-binding protein-1 (p-4E-BP1) (1:300) (Santa Cruz Biotechnology, Santa Cruz, CA); p-p53 (Ser15) (1:1,000) and p53 (1:1,000) (Dako, Denmark); poly-ADP-ribose polymerase (PARP) (1: 1,000) (BD Biosciences); 4E-BP1, p-eukaryotic initiation factor 4E (p-eIF4E) (Ser 209), eIF4E, p-eIF4G (Ser1108), eIF4G, p-Akt (Thr 308), Akt, PIM1, PIM2, PIM3, acetylated(Ac)-H3 histone (Lys 9), Ac-H4 histone, H3 histone and c-Myc (1:1,000) (Cell Signaling Technology); Ac-p53 and Ac-α-tubulin (Lys 40) (1:3,000), vinculin and β-actin (1:1,000) (Sigma-Aldrich, Seattle, WA); H4 histone (1:1,000) (Abcam, Cambridge,
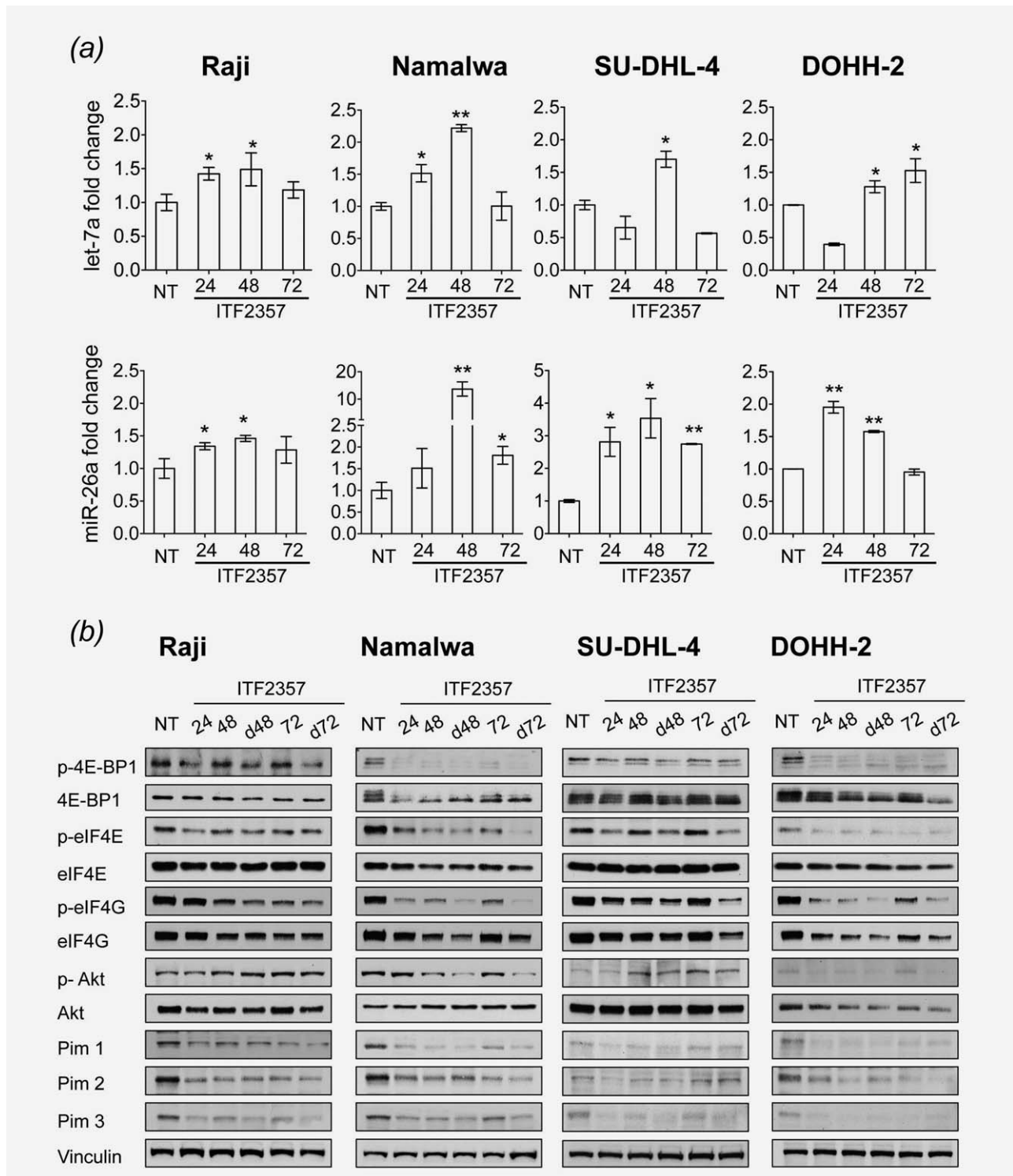
Figure 3. Expression of c-Myc-regulating miRNAs and cap-dependent translation initiation machinery in ITF2357-treated B-NHL cell lines. (*a*) Expression of let-7a (top) and miR-26a (bottom) in Raji, Namalwa, SU-DHL-4 and DOHH-2 cells incubated for the indicated hours with 0.2 μM ITF2357, or untreated as control (NT). Data are shown as fold change in miRNA expression levels relative to the one found in untreated cultures for each time point and represent the mean ± SE of three independent experiments. Significant differences between treated and untreated samples at any time point were calculated with the unpaired two-tailed Student's *t* test (*$P < 0.05$, ** $P < 0.01$). (*b*) Representative western blot analyses of cap-dependent translation initiation complex and its molecular regulators in Raji, Namalwa, SU-DHL-4 and DOHH-2 cells cultured in the absence (NT) or presence of 0.2 μM ITF2357 administered once or every 24 hr (daily, d) for the indicated hours. Cellular vinculin content is shown as an internal protein loading control. Images were acquired by using Microtek ArtixScan F1, and cropped to retain the relevant bands with Adobe Photoshop CS version 4 for Macintosh computer.
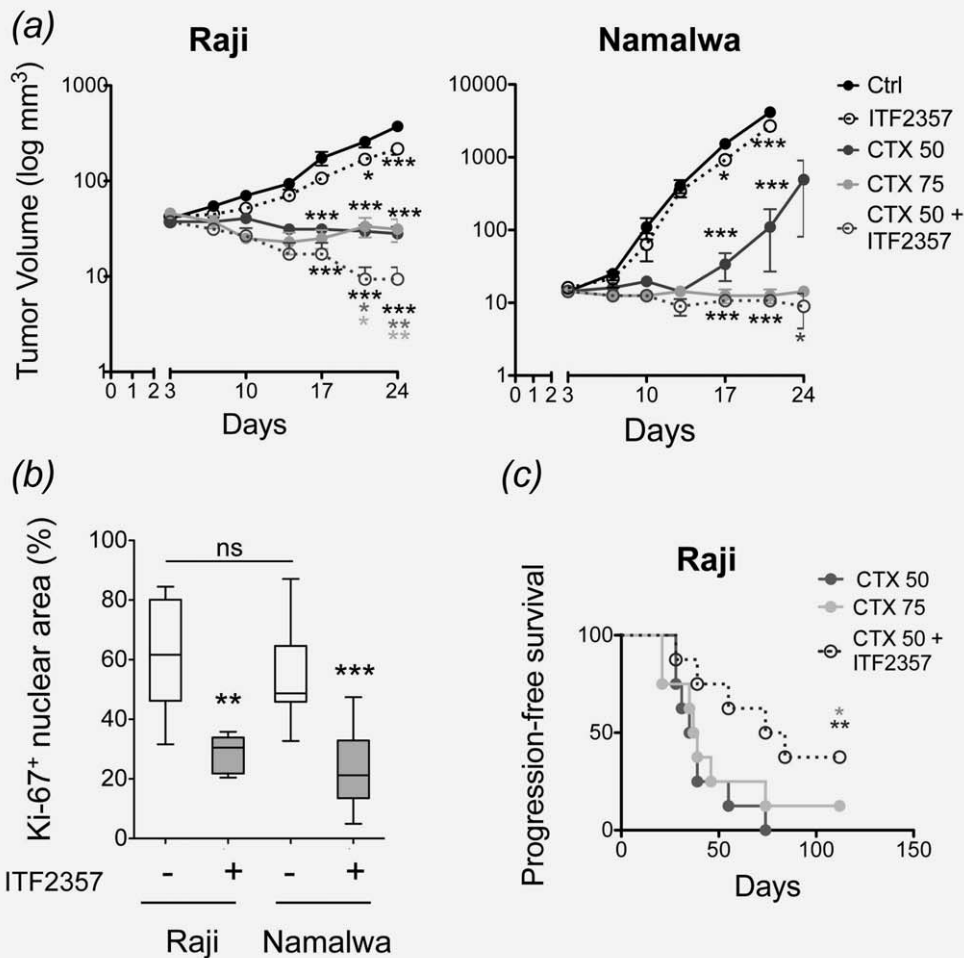
Figure 4. *In vivo* anti-lymphoma activity of ITF2357 in combination with CTX. (*a*) Growth of subcutaneous Raji (left) and Namalwa (right) tumors in SCID mice treated for 3 weeks with CTX following an optimal (75 mg/kg/week, light gray) or a suboptimal (50 mg/kg/week, dark gray) schedule, or with ITF2357 alone (50 mg/kg/day, dotted black) or in combination with suboptimal CTX (CTX 50 + ITF2357, dotted gray) or with saline as control (black). Data show the average tumor volumes ± SE of 8 (Raji) or 7 (Namalwa) mice treated in each group from one out of two independent experiments. Statistically significant differences in treated compared with untreated animals (black asterisks) and between CTX 50− or CTX 75− and CTX 50+ ITF2357-treated groups (dark and light gray asterisks, respectively) were calculated by using the two-way ANOVA (*$P < 0.05$; ** $P < 0.01$; *** $P < 0.001$). (*b*) Ratio between Ki-67-immunostained area and the total nuclear area, measured by ImageJ software analysis version146 in five high-power microscopic fields of tumor sections from ITF2357-treated (+) and control (−) biopsies. The boxes extend from the 25th to the 75th percentiles, the lines indicate the median values, and the whiskers indicate the range of values. Significant differences between treated and untreated samples were calculated with the unpaired two-tailed Student's *t* test (**$P < 0.01$; ***$P < 0.001$; ns, not significant). (*c*) Progression-free survival curves of Raji-xenografted mice treated for 3 weeks with optimal (CTX 75, light gray), or suboptimal (CTX 50, dark gray) CTX or the combination CTX 50 + ITF2357 (dotted gray), which were monitored for up to 112 days for disease recurrence. Statistically significant differences between CTX 50− or CTX 75− and CTX 50+ ITF2357-treated groups (dark and light gray asterisks, respectively) were calculated by using the log rank test (*$P < 0.05$; ** $P < 0.01$).

UK). Membranes were then incubated with the appropriate HRP-conjugated secondary Abs (Amersham) in blocking solution, and signals were visualized with an enhanced ECL system (GE Healthcare) according to the manufacturer's protocol.

RNA extraction, reverse transcription and real-time quantitative PCR analysis

Total RNA was extracted by using Trizol reagent (Invitrogen). Total RNA was reverse-transcribed using Super-Script III reagents (Invitrogen). Levels of c-Myc transcript were nor-malized relative to glyceraldehyde-3-phosphate dehydrogenase (GAPDH), β-actin or hypoxanthine-guanine phosphoribosyltransferase (HPRT) mRNA by using the appropriate TaqMan probes (Applied Biosystems).

To detect and quantify mature miRNAs, the TaqMan MicroRNA Reverse Transcription Kit (Applied Biosystems) was used according to the manufacturer's protocol.

Real time quantitative PCR (qRT-PCR) was carried out in an ABI PRISM 7900 machine (Applied Biosystems). Data were analyzed by applying the $2^{(-\Delta C_t)}$ calculation method.

Table 1. Antitumor effects of ITF2357 and/or CTX in SCID mice xenotransplanted with human BL cell lines

Drug[1]	Dose (mg/kg)	Schedule	Namalwa			Raji		
			Max TVI%[2] (day)	Tox/Tot[3] (day)	CR[4] (day)	Max TWI%[2] (day)	Tox/Tot[3] (day)	CR[4] (day)
ITF2357	50	qdx5/wx6w	42.7 (24)	0/7	0/7 (24)	50.6 (35)	0/8	0/8 (55)
CTX	75	q7dx3	99.6 (24)	0/7	1/7 (17)	98.6 (39)	2/8 (31, 39)	1/8 (112)
CTX	50	q7dx3	97.8 (17)	0/7	0/7 (24)	95.4 (39)	0/8	0/8 (74)
ITF2357	50	qdx5/wx6w	99.9 (24)	0/7	4/7 (24)	99.2 (39)	0/8	5/8 (35)
+ CTX	50	q7dx3						

[1]CTX was dissolved in saline; ITF2357 in DMSO:cremophor:PBS (10:5:85).
[2]MaxTVI, percentage of maximum tumor volume inhibition; in brackets, the day after tumor inoculums.
[3]Tox/Tot, any death in treated mice occurring before any in control mice; in brackets, the day after tumor inoculums.
[4]CR, complete tumor regression lasting at least 1 week.

miRNA inhibition

For miRNA inhibition, 3×10^5 cells (Raji, SU-DHL-4 and DOHH-2) were transiently transfected with LNA-let-7a, or LNA-miR-26a, or a negative control (Exiqon) at a final concentration of 100 nM by using the SiPort Neo-FX reagent (Ambion, Austin, TX) according to the manufacturer's instructions. After 18 hr, cells were treated or not with 0.2 μM ITF2357 for additional 24 or 48 hr, and then processed for miRNA detection by qRT-PCR and c-Myc evaluation by western blot.

In vivo experiments

Severe combined immunodeficiency mice (SCID) (Charles River) were subcutaneously injected with 10×10^6 tumor cells, and, when tumor volumes reached about 50 mm,[3] treated with 0.9% NaCl, 50 mg/kg ITF2357 (5 daily oral administrations/week), 75 (optimal) or 50 (suboptimal) mg/kg CTX (1 injection/week) or 50mg/kg CTX plus ITF2357 for 3 weeks. Mice were then sacrificed, tumor xenografts excised and processed for western blot, qRT-PCR and immunohistochemistry (IHC) analyses. Briefly, formalin-fixed and paraffin-embedded tissue sections, after antigen retrieval in citrate buffer (Novocastra, UK), were incubated overnight with mouse anti-human Ki67 mAb (Dako, Denmark). Immunostaining was revealed with the polymer detection kit (Novocastra) and 3,31-Diaminobenzidine as chromogenic substrate. Tissue sections were lastly counterstained with Harris hematoxylin (Novocastra).

Experimental protocols were approved by the Ethical Committee for Animal Experimentation of the Fondazione IRCCS Istituto Nazionale per lo Studio e la Cura dei Tumori (Milan, Italy), according to the Italian legislation (Legislative Order No. 116 of 1992, as amended), which implements the EU 86/109 Directive.

Statistical analyses

Two-sided Student's *t* test and two-way ANOVA with Bonferroni post-test were used to detect statistically significant differences. Significant differences in disease recurrence between treatment groups were assessed by the log rank test. Pearson correlation coefficient was calculated to measure dependence between variables. Statistical analyses were performed on the Prism 5.0a software (GraphPad Software) version for Macintosh Pro personal computer.

Results

Cytostatic and cytotoxic in vitro activity of ITF2357 against c-Myc+ B-NHL cell lines

We tested the antitumor activity of ITF2357 on human BL (Namalwa and Raji), DLBCL (SU-DHL-4) and FL (DOHH-2) cell lines that overexpress c-Myc (Supporting Information Fig. S1) as a consequence of genetic abnormalities, including translocation under Ig promoter regions (Namalwa, Raji and DOHH-2), and mutations conferring c-Myc protein stabilization (Raji),[17] or post-transcriptional alterations (SU-DHL-4).[28] *In vitro* treatment with increasing concentrations of ITF2357 (0–0.8 μM) resulted in a time- and dose-dependent cell-growth delay, and after 48-hr incubation the average IC50 was approximately 0.2 μM, as measured by a standard 3-(4,5-dimethylthiazol-2-yl)-2,5-diphenyltetrazolium assay (data not shown). The subsequent *in vitro* experiments were thus performed using ITF2357 at 0.2 μM, as a single or daily treatment, in view of the transient HDAC inhibition provided by this compound.[29]

A single administration of 0.2 μM ITF2357 almost completely blocked proliferation in all cell lines for at least 72 hr, with DOHH-2, Namalwa, SU-DHL-4 and Raji displaying respectively $86 \pm 2\%$, $83 \pm 2\%$, $79 \pm 1\%$, $69 \pm 3\%$ growth inhibition after 72 hr (Fig. 1 left). This effect was associated with a rapid cell-cycle arrest in the G1 phase (Fig. 1 middle, dark gray), which in Raji and SU-DHL-4 cultures significantly persisted for up to 144 hr in the absence of daily retreatment. DOHH-2 and Namalwa cells, which experienced a less persistent cell-cycle arrest, were instead the most sensitive to the cytotoxic effects of ITF2357 (Fig. 1 right). Interestingly, daily retreatment also extensively killed SU-DHL-4
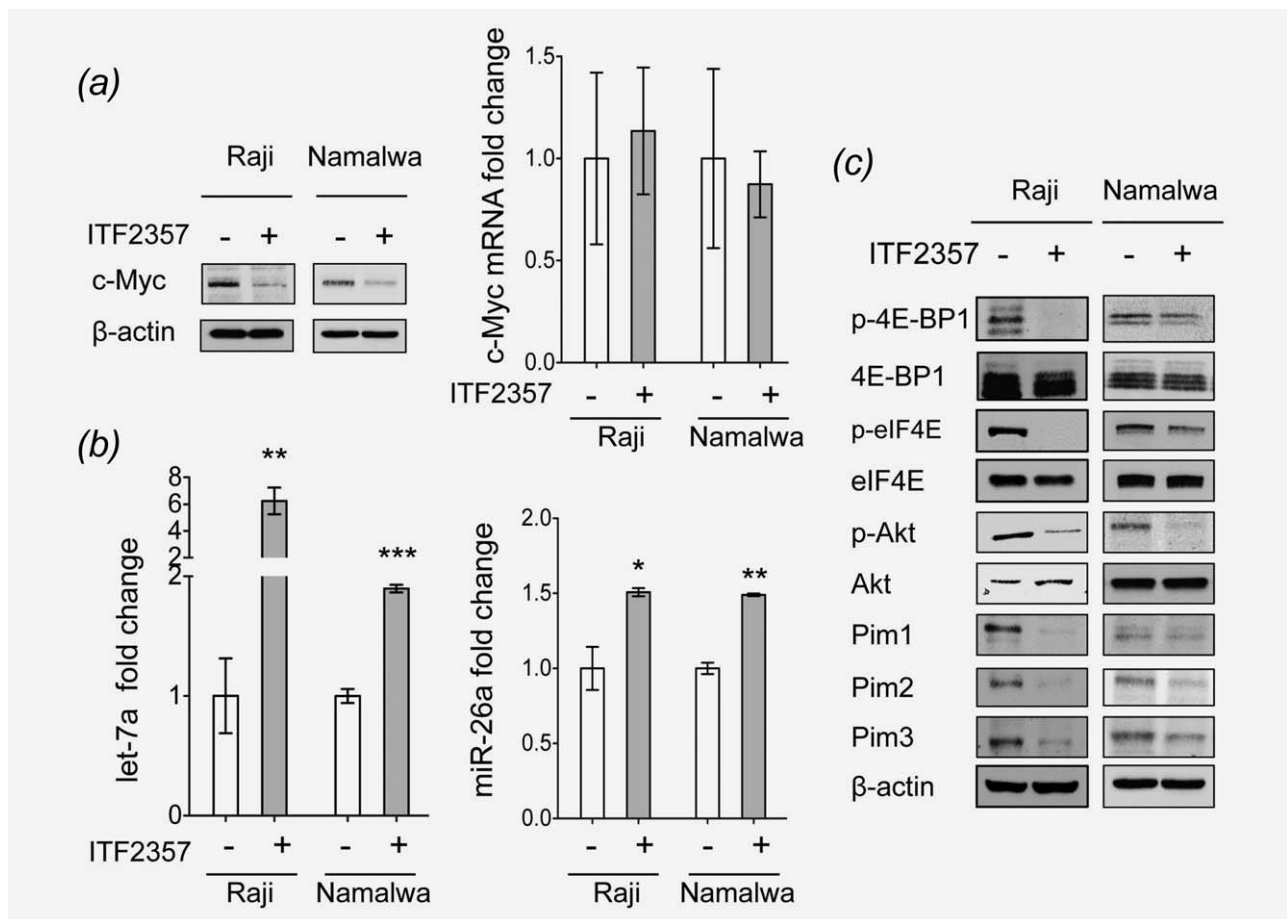
Figure 5. *In vivo* ITF2357-mediated anti-lymphoma effects. Expression of (*a*) c-Myc protein (left) and mRNA (right), (*b*) let-7a (left) and miR-26a (right) and (*c*) activation status of cap-dependent translation initiation machinery and its upstream regulatory molecules in pooled ITF2357-treated (+) or control (−) tumor biopsies, harvested from Raji- and Namalwa-xenografted mice after 3 weeks of treatment. Significant differences between treated and untreated samples were calculated with the unpaired two-tailed Student's *t* test (*$P < 0.05$; **$P < 0.01$; ***$P < 0.00$).

cells, but was not able to significantly boost apoptosis in Raji cultures (Fig. 1 right).

ITF2357-mediated modulation of cytostatic and pro-apoptotic molecular signals

The cytostatic and cytotoxic effects of ITF2357 were confirmed by p21 and p27 upregulation and PARP cleavage induction in treated compared with untreated cultures (Fig. 2*a*). The kinetic of the latter event, in particular, reflected the different ITF2357 sensitivity of the cell lines tested, with Namalwa and DOHH-2 cells more persistently showing cleaved PARP after a single drug administration, SU-DHL-4 and Raji—the latter to a more limited extent—only in case of daily retreatment (Fig. 2*a*). None of these effects seemed to be related to the activation of p53, as they were not associated with either its stabilization or increased phosphorylation at Ser15 (Fig. 2*a*). Accordingly, despite an augmented acetylation level of both nuclear and cytoplasmic proteins in treated cells (Supporting Information Fig. S2), the fraction of acetylated p53 tended to decrease (Fig. 2*a*). The cytostatic and

cytotoxic effects of ITF2357 appeared instead to be more closely associated with c-Myc reduction (Fig. 2*a* and Supporting Information Fig. S3*a*). Indeed, the extent of c-Myc protein downregulation in ITF2357-treated lymphoma cell lines positively correlated with PARP cleavage at all time points, and was thus associated with their sensitivity to ITF2357 pro-apoptotic activity (Pearson $r = 0.6449$, $P = 0.0021$, Supporting Information Fig. S4*a*). In addition, 72 hr after a single administration of ITF2357, which approximately marked the end of its antitumor activity (Fig. 1, left), the degree of c-Myc protein down-modulation (Supporting Information Fig. S3*a*; Raji: $54 \pm 7\%$; SU-DHL-4: $69 \pm 6\%$; Namalwa: $79 \pm 4\%$; DOHH-2: $92 \pm 8\%$) positively correlated with the extent of growth inhibition in lymphoma cultures (Person $r = 0.9807$, $P = 0.0193$, Supporting Information Fig. 4*b*). This indicates that, in c-Myc+ B-NHLs, ITF2357 exerts its antitumor effects in function of its ability of impairing c-Myc expression, and points to c-Myc downregulation as a potential useful biomarker for its activity. ITF2357-mediated reduction of c-Myc expression does not appear to depend on the presence

of a *C-MYC-IG* translocation, but may be hampered when the stable c-Myc(T58A) mutant is expressed, as occurs in Raji cells,[17] in which extensively daily retreatment was required to induce this effect. Interestingly, c-Myc mRNA did not significantly decrease after treatment (Fig. 2*b,* Supporting Information Fig. S3*b*), pointing to ITF2357's ability of preferentially altering the post-transcriptional regulation of c-Myc expression.

ITF2357 interference with the post-transcriptional control of c-Myc expression

To find out the molecular pathways involved in ITF2357-mediated post-transcriptional c-Myc downregulation, we initially determined whether ITF2357 specifically alters the expression of let-7a and miR-26a, the most relevant miRNAs in the control of c-Myc expression.[14,22,23] Indeed, c-Myc constitutes a direct target of translation inhibition mediated by let-7a,[23] and the final target in one of its crucial positive forward loop blocked by miR-26a.[14] Interestingly, in all cellular models, both miRNAs were significantly up-regulated for at least 48 hr after a single treatment (Fig. 3*a*). To further document the significance of this effect, we found that interfering with these miRNAs partially rescued c-Myc downregulation induced by ITF2357 (Supporting Information Fig. S5).

As an additional mechanism that could account for c-Myc post-transcriptional repression, we then investigated whether ITF2357 also altered the activation status of the cap-dependent translation initiation machinery, which is known to specifically control c-Myc protein expression.[25] This process is activated by the transfer of m^7G-cap-binding protein eIF4E from its repressor 4E-BP1 to eIF4G, the central scaffold protein of the eIF4F translation initiation complex, where their further phosphorylation stabilizes the interactions required for correct positioning of ribosomal subunits on the m^7G-cap of mRNA and translation initiation.[30] Akt and PIM kinases are the best-defined signaling hubs regulating cap-dependent translation.[31] Upon mTOR activation, Akt phosphorylates and inactivates 4E-BP1.[30] On the other hand, PIM kinases increase eIF4E expression and phosphorylation.[31] Noteworthy, in all cell lines, ITF2357 reduced the phosphorylation status of 4E-BP1, eIF4E and eIF4G as well (Fig. 3*b* and Supporting Information Fig. S6). Once again, the degree of these effects was associated with the extent of c-Myc downregulation and PARP cleavage in ITF2357-treated cells. In particular, Namalwa and DOHH-2 also most persistently deactivated these proteins after a single ITF2357 administration, whereas Raji and SU-DHL-4 cells most often required daily retreatment (Fig. 3*b* and Supporting Information Fig. S6). Intriguingly, the expression levels of eIF4G total protein also decreased in all cell lines, whereas those of 4E-BP1 and eIF4E specifically decreased in Namalwa and DOHH-2 cells (Fig. 3*b*). To clarify how ITF2357 was able to affect cap-dependent translation, we looked to see whether it altered the expression and activation of its major regulators. In all cell lines, a single treatment potently decreased the expression

levels of all three PIM kinase isoforms, whereas it was not always associated with Akt dephosphorylation (Fig. 3*b*). However, the last effect could not explain the different sensitivity to ITF2357, as phospho-Akt was also being expressed in daily retreated SU-DHL-4 (Fig. 3*b*), which displayed high level of PARP cleavage and apoptosis (Figs. 1, 2*a*). Accordingly, even in the case of no reduction in phospho-Akt, inhibition of eIF4E and eIF4G was still achieved (Fig. 3*b*), probably due to the continuous inhibition of PIM kinases that control cap-dependent translation at a more downstream level compared with the PI3K/Akt/mTOR pathway.[31,32]

These results illustrate the ability of ITF2357 to interfere in different c-Myc+ B-cell NHL histotypes with the two major post-transcriptional regulators of protein expression—namely miRNAs and cap-dependent translation—that are specifically required for the tight control of c-Myc.

In vivo anti-lymphoma effects of ITF2357 in combination with standard chemotherapy

We then verified whether the effects demonstrated *in vitro* by ITF2357 enhanced the *in vivo* anti-lymphoma activity of conventional chemotherapy. SCID mice with sizable subcutaneous Raji or Namalwa tumors were treated daily for 3 weeks with ITF2357 alone or in combination with three courses of a suboptimal dose (50 mg/kg) of CTX. As controls, other groups received in parallel saline or CTX at optimal (75 mg/kg) or suboptimal (50 mg/kg) dose alone. The dosage and schedule of ITF2357 administration was chosen in the light of preliminary experiments showing that, under these conditions, it was well tolerated with no signs of toxicity (data not shown). Accordingly, no significant body-weight loss and no death occurred in ITF2357-treated mice earlier than in the controls (Table 1). In comparison with untreated mice, ITF2357 significantly delayed the *in vivo* growth of both Raji and Namalwa cells and led to a 50.6% and 42.7% reduction in tumor burden respectively after 3 weeks (Table 1, Fig. 4*a*, dotted black line versus black line). This was associated with a significant downregulation of Ki-67 expression, highlighting the capability of the drug to hamper the growing potential of both these highly aggressive lymphomas (Fig. 4*b*, Supporting Information Fig. S7).

Full-dose CTX completely inhibited lymphoma growth (Fig. 4*a* light gray lines), but was not able to eradicate the disease in the most animals (Table 1). Treatment with suboptimal CTX dose was only able to control tumor growth to a similar extent in Raji-xenografted mice; indeed, after the second course, Namalwa nodules started to increase exponentially (Fig. 4*a* right, dark gray line). Addition of ITF2357 significantly enhanced the therapeutic effects of low-dose CTX in both models (Fig. 4*a*, dotted gray line versus dark gray lines), where the combination brought about a complete response (CR) in 60% of mice (Table 1). Furthermore, in Raji-xenografted mice, where low-dose CTX was sufficient to block tumor growth, this combination also compared favorably with optimal CTX alone (Fig. 4*a* left, dotted gray versus

light gray line). The slower *in vivo* engraftment of Raji compared to Namalwa cells (Fig. 4*a*, black lines), despite a comparably marked and widespread Ki-67 positivity (Fig. 4*b*, Supporting Information Fig. S7) which indicates their susceptibility to the cytotoxic effect of an alkylating agent, may provide one explanation for the different outcome of low-dose CTX, and, in turn, its combination with ITF2357 in these models.

The limited tumor burden in Raji-xenografted mice after 3 weeks of treatment with either optimal or suboptimal CTX or its combination with ITF2357 allowed monitoring of tumor growth for an additional 13 weeks. Mice that had received the combination were treated with ITF2357 alone for a further 3 weeks. This resulted in complete disease eradication in 37.5% of the animals, which remained disease free at 112 days after tumor injection (Fig. 4*c*, dotted dark gray line), in sharp contrast with CTX, which, even at the highest dose, reached a long-lasting disease stabilization only in one case (Fig. 4*c*, light gray line).

In line with the *in vitro* findings, *in vivo* treatment with ITF2357 resulted in c-Myc downregulation at protein (Fig. 5*a* left), but not mRNA level (Fig. 5*a* right), induction of let-7a (Fig. 5*b* left; Raji, $P = 0.0013$; Namalwa, $P < 0.0001$) and miR-26a (Fig. 5*b* right; Raji, $P = 0.03$; Namalwa, $P = 0.001$), and reduction of 4E-BP1 and eIF4E phosphorylation in both the models analyzed (Fig. 5*c*). Daily exposure to ITF2357 for 21 days *in vivo* might have favored the occurrence of these molecular effects also in Raji cells, which in this condition displayed similarly marked molecular modulations with respect to Namalwa xenografts (Fig. 5). In addition, not only the expression of PIM kinases, but also Akt phosphorylation was significantly downregulated in both Namalwa and Raji treated biopsies (Fig. 5*c*), highlighting the ability of ITF2357 treatment to interfere *in vivo* with both mechanisms that positively control cap-dependent translation initiation.

Discussion

Our study demonstrates that the pan-HDAC inhibitor ITF2357 potently down-regulates c-Myc protein expression in a panel of human c-Myc-overexpressing B-NHL cell lines independently from the presence of a *C-MYC* translocation. This effect led inevitably to cell-cycle arrest, and correlated with apoptosis induction and cell-growth inhibition. The concurrent induction of let-7a and miR-26a and inhibition of cap-dependent translation initiation machinery provides some explanations of the persistent c-Myc repression after ITF2357 treatment. *In vivo* administration of ITF2357 significantly delayed the growth of human BL xenografts, and its combination with a suboptimal CTX treatment clearly enhanced the anti-lymphoma activity of either agent used alone, and brought about durable complete remissions.

The effectiveness of suppressing c-Myc as an anti-lymphoma option has been widely established;[10,19,33] however, its direct pharmacologic inhibition has remained elusive due to the absence of a defined ligand-binding domain.

Alternative strategies are now focusing on the selective targeting of c-Myc oncogenic functions.[33,34] In this context, the emerging cooperation between c-Myc and HDACs[13–15] indicates that inhibiting these enzymes may turn out to be promising against c-Myc-driven tumors. Recent studies have also revealed the ability of HDAC inhibitors, such as vorinostat, sodium butyrate and depsipeptide to down-regulate not only c-Myc transcriptional activity, but also c-Myc expression itself in both hematologic and solid malignancies, thus constituting a double-edged sword against c-Myc-overexpressing malignancies.[20,21] Building upon the finding that HDAC7 binding to the *C-MYC* genetic sequence is required for its efficient transcription,[35] the possibility that HDACs directly regulate the chromatin architecture of *C-MYC* has been proposed as a mechanism accounting for its downregulation following their inhibition.

However, in all c-Myc+ B-NHL cell lines tested in this study, we show that ITF2357 reduces c-Myc protein but not mRNA levels, through at least two mechanisms: upregulation of the c-Myc-regulating miRNAs let-7a and miR-26a and inhibition of the molecular pathway required for its translation. Several findings point to a greater sensitivity of c-Myc expression to miRNAs-mediated impairment of protein synthesis rather than transcript stability, as demonstrated by (*i*) the lack of a perfect complementarity between c-Myc mRNA and its major regulatory miRNA, let-7a, a condition that usually favors the induction of mRNA degradation;[23] (*ii*) the presence of c-Myc mRNA-miRNA complexes almost exclusively within functional polysomes and not in translationally inactive subpolysomal particles, where mRNA cleavage usually happens;[24,36] (*iii*) and further recent evidence that miRNAs-mediated c-Myc repression occurs at a translation post-initiation phase.[37] In keeping with our results, previous reports have shown that let-7a and miR-26a are widely repressed in tumors overexpressing c-Myc,[22,23] and that their upregulation in aggressive human B-NHL cell lines, including those used in this study, is associated with c-Myc inhibition and cell-growth arrest.[14,16,23,24,38] Whereas let-7a directly targets c-Myc, miR-26a is a key node of a more complex loop regulating c-Myc expression, as it represses the methyltransferase EZH2 thereby releasing its inhibition on miR-494, a recently described c-Myc-targeting miRNA.[14] To ensures its constitutive expression and maintain its lymphomagenic program, c-Myc counteracts this circuit by directly repressing miR-26a, thus disinhibiting EZH2 and blocking miR-494 expression. Increasing evidence is pointing to a crucial pro-oncogenic role of EZH2 in germinal-center-derived B-NHLs,[39] where its concurrent inhibition with c-Myc results in a synergic antitumor effect associated with miR-26a restoration.[16] Even if we cannot rule out that in our models miR-26a induction is the consequence of c-Myc downregulation by other mechanisms here described, this effect may strengthen the level of c-Myc inhibition and at the same time counteract a well-established pro-lymphomagenic circuit. On the other hand, the observation that miRNA genes are also

controlled by epigenetic modulations[14–16,40] raises the hypothesis that miRNA induction after ITF2357 treatment is a consequence of the direct promotion of histone acetylation at their loci.

Nonetheless, interfering with let-7a and miR-26a did not completely rescue the ability of ITF2357 to inhibit c-Myc expression, pointing to the potential concurrent blockade of c-Myc protein synthesis. In line with our hypothesis, we found that ITF2357 significantly impaired the processes leading to c-Myc protein synthesis and stabilization, thus reinforcing its anti-Myc activity. In cancer, activation of cap-dependent translation via eIF4E de-repression and binding to eIF4G within the eIF4F translation initiation complex, coupled with the concurrent phosphorylation of these molecules, ensures the production of short-lived oncoproteins, including c-Myc.[25] PI3K/Akt/mTOR axis and, further downstream, PIM kinases are the key regulators of cap-dependent translation activation.[41] Besides their common ability of activating c-Myc translation, these molecules favor c-Myc protein stability[42,43] and genetic transactivation,[12] thus contributing at several levels to c-Myc overexpression. In keeping with this finding, a wide body of evidence is highlighting their crucial involvement in c-Myc-driven lymphomagenesis, as the activation of either PI3K,[44] PIM kinases,[32,41] or eIF4E[45] significantly accelerate tumor formation in Eµ-*MYC* models, indicating a pro-lymphoma cooperation between c-Myc overexpression and these pathways. Interestingly, PIM kinases are specifically overexpressed in FL,[41] DLBCL[46] and mantle cell lymphoma[47] with a poor response to conventional treatments and have thus been proposed as potential valuable therapeutic targets in these diseases. In this context, the ability of ITF2357 to down-modulate all PIM kinases, deactivate key components of the cap-dependent translation initiation machinery while promoting 4E-BP1 inhibitory functions in different aggressive B-NHL models highlights its substantial therapeutic potential. Given the addiction of cancer cells to cap-dependent translation, inhibition of this process at the most downstream level by ITF2357 might constitute a useful therapeutic option to counteract the aberrant PI3K/Akt/mTOR signaling cascade commonly activated in B-NHLs[44,48] and sensitize tumor cells to apoptosis. Accordingly, in all lymphoma cell lines tested in our study, ITF2357 reduced the activity of cap-dependent translation even when Akt was not inhibited.

At present, we can only speculate about the potential mechanisms through which ITF2357 inhibits PIM kinases. Nonetheless, all the reported levels of control for their expression may be in principle affected by ITF2357. Indeed, protein synthesis of PIM kinases requires the activity of cap-dependent translation, and their stability the presence of

molecular chaperones and the downregulation of specific miR-NAs.[32] We have demonstrated that ITF2357 inhibits cap-dependent translation and alters the miRNA expression pattern, whereas the function of HDAC inhibition to impair heat shock protein 90 chaperone activity has been extensively reported,[49] thus providing an initial explanation for ITF2357's ability to repress PIM kinases. This finding for the first time indicates that the reported difficulties of developing a unique PIM kinase inhibitor[32] might be easily overcome by using a pan-HDAC inhibitor that is already clinically available.[50]

All together these ITF2357-mediated molecular effects significantly enhanced the *in vivo* anti-lymphoma activity of a suboptimal and well-tolerated dose of CTX, bringing its efficacy at least to the level of the optimal treatment, while reducing its toxicity. The possibility to further extend the therapeutic potential of this combination seems to rely on the capability of the chemotherapeutic agent to control the *in vivo* lymphoma growth.

In conclusion, at least in the context of c-Myc+ human B-NHLs, ITF2357 treatment provides significant anti-lymphoma effects in association with its many-sided ability to counteract c-Myc overexpression, which can thus be considered as a reliable biomarker for its activity. This, however, does not exclude the effectiveness of ITF2357 against other oncotypes, considering that the pleiotropic effects of HDAC inhibitors strictly rely on the biologic context they encounter. Even though the mechanisms through which ITF2357 consistently induces let-7a and miR-26a, and inhibits PIM kinases and cap-dependent translation in Myc+ B-NHLs are not fully elucidated, the opportunity to provide all these effects with a single agent may be of a substantial therapeutic advantage, given that they have already demonstrated a significant anti-lymphoma activity individually.[16,23,38,41,45] For these reasons, ITF2357 may constitute a valuable addition to conventional anti-lymphoma chemotherapy for the treatment of the still very ominous c-Myc-overexpressing B-NHLs.[6–8] In addition, our findings highlight the importance of testing the therapeutic advantages of ITF2357 in combination with the wide array of novel agents able to interfere with the PI3K/Akt/mTOR pathway and/or EZH2 activity, which significantly boost c-Myc-driven lymphomagenesis.[44,48]

References

1. Slack GW, Gascoyne RD. MYC and aggressive B-cell lymphomas. *Adv Anat Pathol* 2011;18:219–28.
2. Chng WJ, Huang GF, Chung TH, et al. Clinical and biological implications of MYC activation: a common difference between MGUS and newly diagnosed multiple myeloma. *Leukemia* 2011;25:1026–35.
3. Boxer LM, Dang CV. Translocations involving c-myc and c-myc function. *Oncogene* 2001;20:5595–610.
4. Di Nicola M, Carlo-Stella C, Mariotti J, et al. High response rate and manageable toxicity with an intensive, short-term chemotherapy programme for Burkitt's lymphoma in adults. *Br J Haematol* 2004;126:815–20.

Cancer Cell Biology

5. Molyneux EM, Rochford R, Griffin B, et al. Burkitt's lymphoma. *Lancet* 2012;379:1234–44.

6. Barrans S, Crouch S, Smith A, et al. Rearrangement of MYC is associated with poor prognosis in patients with diffuse large B-cell lymphoma treated in the era of rituximab. *J Clin Oncol* 2010; 28:3360–5.

7. Cuccuini W, Briere J, Mounier N, et al. MYC+ diffuse large B-cell lymphoma is not salvaged by classical R-ICE or R-DHAP followed by BEAM plus autologous stem cell transplantation. *Blood* 2012;119:4619–24.

8. Hartmann E, Fernandez V, Moreno V, et al. Five-gene model to predict survival in mantle-cell lymphoma using frozen or formalin-fixed, paraffin-embedded tissue. *J Clin Oncol* 2008;26:4966–72.

9. Harris AW, Pinkert CA, Crawford M, et al. The E mu-myc transgenic mouse. A model for high-incidence spontaneous lymphoma and leukemia of early B cells. *J Exp Med* 1988;167:353–71.

10. Felsher DW, Bishop JM. Reversible tumorigenesis by MYC in hematopoietic lineages. *Mol Cell* 1999;4:199–207.

11. Li Z, Van Calcar S, Qu C, et al. A global transcriptional regulatory role for c-Myc in Burkitt's lymphoma cells. *Proc Natl Acad Sci USA* 2003; 100:8164–9.

12. Zippo A, De Robertis A, Serafini R, Oliviero S. PIM1-dependent phosphorylation of histone H3 at serine 10 is required for MYC-dependent transcriptional activation and oncogenic transformation. *Nat Cell Biol* 2007;9:932–44.

13. Kurland JF, Tansey WP. Myc-mediated transcriptional repression by recruitment of histone deacetylase. *Cancer Res* 2008;68:3624–9.

14. Zhang X, Zhao X, Fiskus W, et al. Coordinated silencing of MYC-mediated miR-29 by HDAC3 and EZH2 as a therapeutic target of histone modification in aggressive B-cell lymphomas. *Cancer Cell* 2012;22:506–23.

15. Zhang X, Chen X, Lin J, et al. Myc represses miR-15a/miR-16-1 expression through recruitment of HDAC3 in mantle cell and other non-Hodgkin B-cell lymphomas. *Oncogene* 2012;31: 3002–8.

16. Zhao X, Lwin T, Zhang X, et al. Disruption of the MYC-miRNA-EZH2 loop to suppress aggressive B-cell lymphoma survival and clonogenicity. *Leukemia* 2013;27:2341–50.

17. Bahram F, von der Lehr N, Cetinkaya C, et al. c-Myc hot spot mutations in lymphomas result in inefficient ubiquitination and decreased proteasome-mediated turnover. *Blood* 2000;95: 2104–10.

18. Pelengaris S, Khan M, Evan G. c-MYC: more than just a matter of life and death. *Nat Rev Cancer* 2002;2:764–76.

19. Gomez-Curet I, Perkins RS, Bennett R, et al. c-Myc inhibition negatively impacts lymphoma growth. *J Pediatr Surg* 2006;41:207–11; discussion 11.

20. Seo SK, Jin HO, Woo SH, et al. Histone deacetylase inhibitors sensitize human non-small cell lung cancer cells to ionizing radiation through acetyl p53-mediated c-myc down-regulation. *J Thorac Oncol* 2011;6:1313–9.

21. Kretzner L, Scuto A, Dino PM, et al. Combining histone deacetylase inhibitor vorinostat with aurora kinase inhibitors enhances lymphoma cell killing with repression of c-Myc, hTERT, and microRNA levels. *Cancer Res* 2011;71:3912–20.

22. Sander S, Bullinger L. Repressing the repressor: a new mode of MYC action in lymphomagenesis. *Cell Cycle* 2009;8:556–9.

23. Sampson VB, Rong NH, Han J, et al. MicroRNA let-7a down-regulates MYC and reverts MYC-induced growth in Burkitt lymphoma cells. *Cancer Res* 2007;67:9762–70.

24. Kim HH, Kuwano Y, Srikantan S, et al. HuR recruits let-7/RISC to repress c-Myc expression. *Genes Dev* 2009;23:1743–8.

25. Lin CJ, Cencic R, Mills JR, et al. c-Myc and eIF4F are components of a feedforward loop that links transcription and translation. *Cancer Res* 2008;68:5326–34.

26. Zappasodi R, Pupa SM, Ghedini GC, et al. Improved clinical outcome in indolent B-cell lymphoma patients vaccinated with autologous tumor cells experiencing immunogenic death. *Cancer Res* 2010;70:9062–72.

27. Zappasodi R, Bongarzone I, Ghedini GC, et al. Serological identification of HSP105 as a novel non-Hodgkin lymphoma therapeutic target. *Blood* 2011;118:4421–30.

28. Lewis TS, McCormick RS, Stone IJ, et al. Proapoptotic signaling activity of the anti-CD40 monoclonal antibody dacetuzumab circumvents multiple oncogenic transformation events and chemosensitizes NHL cells. *Leukemia* 2011;25: 1007–16.

29. Barbetti V, Gozzini A, Rovida E, et al. Selective anti-leukaemic activity of low-dose histone deacetylase inhibitor ITF2357 on AML1/ETO-positive cells. *Oncogene* 2008;27:1767–78.

30. Sonenberg N, Hinnebusch AG. Regulation of translation initiation in eukaryotes: mechanisms and biological targets. *Cell* 2009;136:731–45.

31. Hammerman PS, Fox CJ, Birnbaum MJ, et al. Pim and Akt oncogenes are independent regulators of hematopoietic cell growth and survival. *Blood* 2005;105:4477–83.

32. Nawijn MC, Alendar A, Berns A. For better or for worse: the role of Pim oncogenes in tumorigenesis. *Nat Rev Cancer* 2011;11:23–34.

33. Mertz JA, Conery AR, Bryant BM, et al. Targeting MYC dependence in cancer by inhibiting BET bromodomains. *Proc Natl Acad Sci USA* 2011;108:16669–74.

34. Kessler JD, Kahle KT, Sun T, et al. A SUMOylation-dependent transcriptional subprogram is required for Myc-driven tumorigenesis. *Science* 2012;335:348–53.

35. Zhu C, Chen Q, Xie Z, et al. The role of histone deacetylase 7 (HDAC7) in cancer cell proliferation: regulation on c-Myc. *J Mol Med* 2011;89: 279–89.

36. Maroney PA, Yu Y, Fisher J, et al. Evidence that microRNAs are associated with translating messenger RNAs in human cells. *Nat Struct Mol Biol* 2006;13:1102–7.

37. Kong YW, Cannell IG, de Moor CH, et al. The mechanism of micro-RNA-mediated translation repression is determined by the promoter of the target gene. *Proc Natl Acad Sci USA* 2008;105: 8866–71.

38. Sander S, Bullinger L, Klapproth K, et al. MYC stimulates EZH2 expression by repression of its negative regulator miR-26a. *Blood* 2008;112:4202–12.

39. Beguelin W, Popovic R, Teater M, et al. EZH2 is required for germinal center formation and somatic EZH2 mutations promote lymphoid transformation. *Cancer Cell* 2013;23:677–92.

40. Sampath D, Liu C, Vasan K, et al. Histone deacetylases mediate the silencing of miR-15a, miR-16, and miR-29b in chronic lymphocytic leukemia. *Blood* 2012;119:1162–72.

41. Schatz JH, Oricchio E, Wolfe AL, et al. Targeting cap-dependent translation blocks converging survival signals by AKT and PIM kinases in lymphoma. *J Exp Med* 2011;208.

42. Zhang Y, Wang Z, Li X, et al. Pim kinase-dependent inhibition of c-Myc degradation. *Oncogene* 2008;27:4809–19.

43. Kumar A, Marques M, Carrera AC. Phosphoinositide 3-kinase activation in late G1 is required for c-Myc stabilization and S phase entry. *Mol Cell Biol* 2006;26:9116–25.

44. Sander S, Calado DP, Srinivasan L, et al. Synergy between PI3K signaling and MYC in Burkitt lymphomagenesis. *Cancer Cell* 2012;22: 167–79.

45. Lin CJ, Nasr Z, Premsrirut PK, et al. Targeting synthetic lethal interactions between Myc and the eIF4F complex impedes tumorigenesis. *Cell Rep* 2012;1:325–33.

46. Gomez-Abad C, Pisonero H, Blanco-Aparicio C, et al. PIM2 inhibition as a rational therapeutic approach in B-cell lymphoma. *Blood* 2011;118: 5517–27.

47. Hsi ED, Jung SH, Lai R, et al. Ki67 and PIM1 expression predict outcome in mantle cell lymphoma treated with high dose therapy, stem cell transplantation and rituximab: a Cancer and Leukemia Group B 59909 correlative science study. *Leuk Lymphoma* 2008;49:2081–90.

48. Schmitz R, Young RM, Ceribelli M, et al. Burkitt lymphoma pathogenesis and therapeutic targets from structural and functional genomics. *Nature* 2012;490:116–20.

49. Rao R, Fiskus W, Yang Y, et al. HDAC6 inhibition enhances 17-AAG-mediated abrogation of hsp90 chaperone function in human leukemia cells. *Blood* 2008;112:1886–93.

50. Furlan A, Monzani V, Reznikov LL, et al. Pharmacokinetics, safety and inducible cytokine responses during a phase 1 trial of the oral histone deacetylase inhibitor ITF2357 (givinostat). *Mol Med* 2011;17:353–62.